Single Amino Acid Substitutions at the N-Terminus of a Recombinant Cytotoxic Ribonuclease Markedly Influence Biochemical and Biological Properties†

Dianne L. Newton,‡ Lluis Boque,§ Alexander Wlodawer,§ Charles Y. Huang,|| and Susanna M. Rybak*,⊥

Intramural Research Support Program, SAIC Frederick, Macromolecular Structure Laboratory, ABL-Basic Research Program, and Laboratory of Biochemical Physiology, Division of Basic Science, National Cancer Institute—Frederick Cancer Research and Development Center, Frederick, Maryland 21702, and Laboratory of Biochemistry, National Heart, Lung and Blood Institute, Bethesda, Maryland 20892

Received August 28, 1997; Revised Manuscript Received December 12, 1997

ABSTRACT: Onconase is a cytotoxic ribonuclease with antitumor properties. A semisynthetic gene encoding the entire protein sequence was constructed by fusing oligonucleotides coding for the first 15 and the last 6 of the 104 amino acids to a genomic clone that encoded the remaining amino acid residues [Newton, D. L., et al. (1997) *Protein Eng. 10*, 463−470]. The resulting protein product expressed in *Escherichia coli* exhibited little enzymatic or cytotoxic activity due to the unprocessed N-terminal Met amino acid residue. In this study, we demonstrate that modification of the 5′-region of the gene to encode [Met-(−1)]Ser or [Met-(−1)]Tyr instead of the native pyroglutamate results in recombinant onconase derivatives with restored activities. [Met-(−1)]rOnc(E1S) was more active than [Met-(−1)]rOnc(E1Y) in all assays tested. Consistent with the action of native onconase, [Met-(−1)]rOnc(E1S) was a potent inhibitor of protein synthesis in the cell-free rabbit reticulocyte lysate assay, degrading tRNA at concentrations that correlated with inhibition of protein synthesis. An interesting difference between the recombinant onconase derivatives and the native protein was their susceptibility to inhibition by the major intracellular RNase inhibitor, PRI (onconase is refractory to PRI inhibition). [Met-(−1)]rOnc(E1S) and [Met-(−1)]rOnc-(E1Y) inhibited protein synthesis in intact SF539 neuroblastoma cells with IC_{50}'s very similar to that of onconase (IC_{50} 3.5, 10, and 10 μg/mL after 1 day and 0.16, 0.35, and 2.5 μg/mL after 5 days for onconase, [Met-(−1)]rOnc(E1S), and [Met-(−1)]rOnc(E1Y), respectively). Similar to that of onconase, cytotoxic activity of the recombinant derivatives was potentiated by monensin, NH_4Cl, and retinoic acid. Brefeldin A completely blocked the enhancement of cytotoxicity caused by retinoic acid with all three proteins. Thus, drug-induced alterations of the intracellular trafficking of the recombinant derivatives also resembles that of onconase. Stability studies as assessed in serum-containing medium in the presence or absence of cells at 37 °C showed that the recombinant proteins were as stable to temperature and cell culture conditions as the native protein. Therefore, exchanging the Glu amino acid residue at the amino terminus of onconase with an amino acid residue containing a hydroxyl group produces recombinant proteins with ribonuclease and cytotoxic properties similar to native onconase.

Onconase, isolated from extracts of *Rana pipiens* oocytes by following cytotoxic effects toward tumor cells (*1*, *2*), is homologous to pancreatic ribonuclease (RNase A)[1] in both primary (*3*) and tertiary amino acid structure (*4*). X-ray crystallographic structure revealed that the N-terminal pyroglutamyl (⟨Glu1) residue forms part of the enzyme active site. The role of the ⟨Glu1 was further confirmed by Boix et al. (*5*), who demonstrated that cleavage of the N-terminal methionine residue of recombinant onconase, [Met-(−1)]-rOnc, with cyanogen bromide and cyclization of the glutamine (Gln1) residue to re-form the ⟨Glul N-terminus reconstituted onconase activities. Thus, the involvement of the N-terminus in the active site of onconase has complicated the expression of recombinant onconase in *Escherichia coli* systems that result in the accumulation of methionine-fusion proteins in inclusion bodies (*5*, *6*). Structural analysis of onconase suggested that the integrity of the active site interactions might be reconstituted if [Met-(−1)]rOnc contained Ser or Tyr at the amino terminus, since the hydroxyl groups in each of these residues could help to form a hydrogen-bonding pattern similar to that in the native enzyme. These derivatives of onconase were engineered, expressed, purified, and characterized. As predicted, the enzymatic and cytotoxic

† This research was sponsored in part by the National Cancer Institute, DHHS, under contract with ABL.

* Corresponding author: Laboratory of Biochemical Physiology, NCI−FCRDC, Building 567, Room 152, Frederick, MD 21702-1201. Telephone: 301/846-5215. Fax: 301/846-6863. E-mail: rybak@ncifcrf.gov.

‡ Intramural Research Support Program, SAIC Frederick, NCI−FCRDC.

§ Macromolecular Structure Laboratory, ABL-Basic Research Program, NCI−FCRDC.

|| National Heart, Lung and Blood Institute.

⊥ Laboratory of Biochemical Physiology, Division of Basic Science, NCI−FCRDC.

[1] Abbreviations: RNase A, pancreatic ribonuclease A; nOnc, native onconase; [Met-(−1)]rOnc, recombinant onconase; [Met-(−1)]rOnc-(E1S), recombinant onconase in which (+1) glutamic acid was changed to serine; [Met-(−1)]rOnc(E1Y), recombinant onconase in which (+1) glutamic acid was changed to tyrosine; PCR, polymerase chain reaction; PRI, placental ribonuclease inhibitor, ⟨Glu1, N-terminal pyroglutamic acid; BFA, brefeldin A.

S0006-2960(97)02147-8
Published on Web 03/26/1998

activities were reconstituted, albeit with some differences compared with the native protein.

Onconase is the first ribonuclease to be evaluated in Phase I and Phase I/II clinical trials as a single therapeutic agent in patients with a variety of solid tumors (*7*). Moreover, conjugation of onconase to cell-type-specific ligands increased its potency toward tumor cells (*8*). Taken together, these results indicate that onconase has properties that may be advantageous for the generation of potent selective cell-killing agents. The relevance of the results presented herein to designing new targeted therapeutics for cancer treatment will be discussed.

MATERIALS AND METHODS

Materials. Native onconase (nOnc) was purified from *Rana pipiens* oocytes obtained from NASCO (Fort Atkinson, WI) following the published protocol (*3*). Antibodies to the denatured proteins were prepared by Assay Research (College Park, MD). Reagents for performing PCR and direct cloning of PCR products were obtained from Perkin-Elmer Corp. (Norwalk, CT) and from Invitrogen (San Diego, CA), respectively. *all-trans*-Retinoic acid, brefeldin A, and monensin were from Sigma (St. Louis, MO). Placental ribonuclease inhibitor (PRI) was from Promega (Madison, WI). Substrates for the ribonuclease assays were purchased from Sigma and Boehringer Mannheim (Indianapolis, IN). The materials (and their sources) used in the construction and expression of the recombinant proteins, cell culture, and rabbit reticulocyte lysate assays are as described in ref *9*.

Design of Mutants and Structural Analysis. Design of the mutants was based on the analysis of the three-dimensional structure of native onconase (*4*) using the program TOM (*10*). Models for all of the recombinant proteins were based on this structure. To analyze the interactions between the different onconase mutants and PRI, the modeled recombinant structures were superimposed on those of the RNase moiety in the PRI−RNase A complex (*11*) and subsequently submitted to energy minimization using program X-PLOR (*12*).

Plasmid Construction and Expression and Protein Purification. The N- and C-termini of the recombinant RNases were reconstructed using the PCR technique of splicing by overlap extension (*13*) with amino acid residues 1−15 of onconase at the N-terminus (position 1 containing either glutamic acid, serine, or tyrosine amino acid residues) and amino acid residues 99−104 of onconase at the C-terminus (*6*). The assembled genes were inserted between the *Xba*I and *Bam*HI sites of the pET-11d bacterial expression vector (Novagen, Madison, WI). All procedures were accomplished essentially as described in ref *9*. The plasmids were expressed in BL21(DE3) *E. coli* cells as recommended by the supplier, Novagen. The recombinant proteins were isolated from inclusion bodies, denatured, renatured, and dialyzed as described (*9*) before being applied to a CM-Sephadex C-50 column (Pharmacia Biotech Inc., Piscataway, NJ). The proteins were eluted with a NaCl gradient (0−0.5 M) in 20 mM Tris-HCl, pH 7.5, containing 10% glycerol. Final purification was achieved by size-exclusion chromatography on Sephadex G-100 equilibrated and eluted with 5% formic acid. The proteins were pooled; dialyzed against 20 mM Tris-HCl, pH 7.5, containing 25 mM NaCl; and lyophilized.

In Vitro Translation Assay and Analysis of RNA. The in vitro translation assay was performed as described previously (*14*). RNA from control or RNase-treated lysates was prepared as described (*14*). Electrophoresis was accomplished by using 10% TBE gels (Novex, San Diego, CA).

Ribonuclease Assay. Ribonuclease activity using high molecular weight RNA and tRNA was determined at 37 °C by monitoring the formation of perchloric acid-soluble nucleotides following published protocols (*9*). The buffers were either 10 mM Hepes, pH 6.0, containing 0.13 mg/mL human serum albumin or 0.16 M Tris-HCl, pH 7.5, containing 1.6 mM EDTA and 0.2 mg/mL human serum albumin. With poly(A,C), UpG, and poly(U), ribonuclease activity was assayed according to refs *15* and *16* by measuring the increase in absorbance at 260 nm with time. Incubation mixtures (1 mL of 10 mM imidazole and 0.1 M NaCl, pH 6.5 or 7.0) contained substrate and appropriate amounts of enzyme solution at 25 °C. Final substrate concentrations in the assays were 0.49 mM for UpG and 0.033, 0.029, and 0.33 mg/mL for poly(U), poly(A,C), and highly polymerized yeast RNA, respectively. Each assay was repeated 2−6 times, and the average value was used in data treatment. Kinetic parameters were obtained with the aid of the data analysis program of Cleland (*17*).

Ribonuclease Inhibitor Interaction. PRI inhibition of [Met-(−1)rOnc(E1Y) and [Met-(−1)]rOnc(E1S) was determined with tRNA as substrate. Substrate concentrations were varied between 0.23 and 3.6 and between 0.35 and 5.7 mg/mL for [Met-(−1)]rOnc(E1Y) and [Met-(-l)]rOnc(E1S), respectively. Usually four different PRI concentrations were used in studying the inhibition of [Met-(−1)]rOnc(E1Y) and [Met-(−1)]rOnc(E1S). The reaction was performed for 2 h at 37 °C in a final volume of 0.3 mL containing 0.17 M Tris-HCl, pH 7.5, 0.17 mM EDTA, 0.17 mg/mL human serum albumin (Calbiochem, San Diego, CA), 1.5 mM DTT, and the appropriate concentrations of PRI and tRNA. The reaction was started by the addition of enzyme (0.32 and 0.1 μM for [Met-(−1)]rOnc(E1Y) and [Met-(−1)]rOnc(E1S), respectively). Assays were terminated with 700 μL of 3.4% ice-cold perchloric acid, and the remaining steps were carried out as described (*9*). Each assay was repeated 2−11 times.

Since the condition of free PRI concentration approximating total concentration ($I_{free} \simeq I_o$) no longer applies in tight-binding situations, we first used the Henderson plot (*18*) to obtain the apparent inhibition constant, K_i',

$$I_o\nu/(\nu - \nu_i) = E_0 + K_i'\nu/\nu_i \quad (1)$$

where ν and ν_i are the activities in the absence and presence of PRI, and E_o is the total enzyme concentration. Depending on the mechanism of inhibition, the value of K_i' may change with respect to the substrate concentration and the magnitude of K_m. However, knowledge of K_i' permitted us to calculate the free PRI concentration according to the relationship

$$I_f = I_o/(1 + E_o\nu_i/K_i'\nu) \quad (2)$$

Knowing I_f, we then determined K_i by the Dixon plot ($1/\nu$ vs I_f).

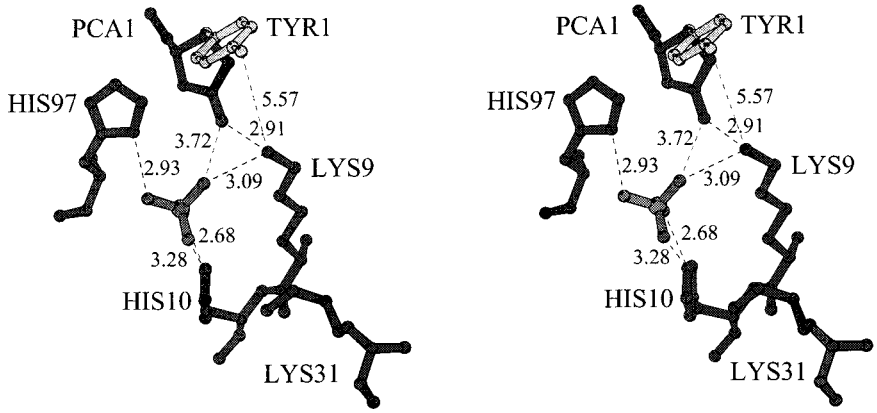

FIGURE 1: Stereographic view of the active site of onconase showing the distances between selected atoms (Å). The central phosphate is shown in gray; the residues corresponding to native onconase, in black; and Tyr1 [corresponding to the mutant [Met-(−1)]rOnc(E1Y)], in gray. The coordinates for nOnc correspond to those reported in ref *4* in which the conformation of Lys31 is not the one expected for an active enzyme. Tyr1 is modeled in the same position as pyroglutamate 1 without further refinement. Even though the OH(Tyr1)−NZ(Lys9) distance is quite large in such a model, the N-terminal portion of the protein may rearrange its conformation to allow the formation of H-bonds between OH(Tyr1) and the other residues in the active site region. A similar situation would occur for the [Met-(−1)]rOnc(E1S) mutant. The side chain of Ser in the (E1S) mutant, without further refinement, would overlap with the side chain of Tyr; therefore, it is not displayed for clarity.

Reductive Methylation. nOnc and [Met-(−1)]rOnc(E1S) were tritiated by using the reductive methylation procedure as described in ref *19*. Tritiated proteins were tested for activity in the rabbit reticulocyte lysate assay and found to express activities identical to those of the unlabeled proteins. The specific activities of tritiated nOnc and [Met-(−1)]rOnc-(E1S) were 16 800 and 2500 dpm/pmol, respectively.

Protein Synthesis Assays in Cultured Cells. Protein synthesis was measured as previously described (*20*). Briefly, cells (0.1 mL, 2.5×10^4 cells/mL) were plated into 96-well microtiter plates in Dulbecco's minimum essential medium supplemented with 10% heat-inactivated fetal bovine serum; additions were made in a total volume of 10 μL, and the plates were incubated at 37 °C for the times indicated. Phosphate-buffered saline (PBS) containing 0.1 mCi of [^{14}C]-leucine was added for 2−4 h, and the cells were harvested onto glass fiber filters by using a PHD cell harvester, washed with water, dried with ethanol, and counted. To examine intracellular routing, retinoic acid (12 mM in DMSO), monensin (1.4 mM in ethanol), and brefeldin A (BFA, 10 mg/mL in ethanol) were diluted into cell culture medium to 10 μM, 0.12 μM, and 4 μg/mL final concentrations, respectively, and the cells were treated as described in ref *21*. The results are expressed as percent of [^{14}C]leucine incorporation in the mock-treated wells.

Stability Assays. The stabilities of nOnc vs [Met-(−1)]-rOnc(E1S) and [Met-(−1)]rOnc(E1Y) were determined by incubating them as prediluted concentration curves in 96-well plates at 37 °C in Dulbecco's minimum essential medium supplemented with 10% heat-inactivated fetal bovine serum for 0, 2, and 4 days. The amount of active protein remaining was determined by transferring the media containing the dilutions to 96-well plates containing untreated adherent SF539 cells and determining cytotoxicity after 72 additional hours in culture. The dilutions for the dose response curves were also incubated in 96-well plates containing adherent SF539 cells in the presence of complete growth medium. For these experiments, the amount of active protein remaining was determined by transferring those dilutions to 96-well plates containing untreated adherent SF539 cells and determining cytotoxicity.

To measure degradation of tritiated protein, SF539 cells (1.8×10^5 cells) were plated into 30-mm tissue culture dishes 24 h prior to treatment. [^{3}H]nOnc (1.7×10^4 dpm/pmol) or [^{3}H][Met-(−1)]rOnc(E1S) (2.5×10^3 dpm/pmol) was added at a final concentration of 3 μg/mL, and the plates were incubated at 37 °C for 48 or 72 h in the absence or presence of serum, respectively. Aliquots (500 μL) were removed at 0, 24, 48, and 72 h as appropriate, and the level of proteolysis was determined by measuring acid-soluble radioactivity. Precipitation of acid-insoluble radioactivity was accomplished by using 3.25% phosphotungstate in 5% HCl as previously described (*19*).

RESULTS

Designing and Modeling Novel rOnc Proteins. Models were built of recombinant onconase ([Met-(−1)rOnc) and of two derivatives with changes in the N-terminal amino acid following the initiating methionine. Serine [Met-(−1)]rOnc-(E1S) and tyrosine [Met-(−1)]rOnc(E1Y) were based on the coordinates of nOnc (*4*) and subjected to regularization using the program TOM (*10*). The models for the different structures look very similar overall, but the mutations affect a region very close to the active site. The direct superposition of those residues in the position of ⟨Glu shows that Tyr1 would be close enough to hydrogen bond directly to Lys9 and to the phosphate group in the active site by means of a small displacement of the N-terminal residues (Figure 1) or to interact with Lys9 through a water molecule without any further displacement. In the case of Ser, a slightly larger rearrangement of this region would be needed to allow such contacts to be formed.

Models created for the complexes between PRI and the different onconase variants indicated that the N-terminal region of onconase, in addition to being close to the active site, is also in the interface with PRI (not shown).

Cloning and Expression of rOnc Derivatives. The gene for [Met-(−1)]rOnc comprises a *R. pipiens* genomic DNA segment encoding native onconase (nOnc) from amino acid residues 16−98 with amino acid residues 1−15 and 99−104 encoded by synthetic oligonucleotides (*6*). Oligonucle-

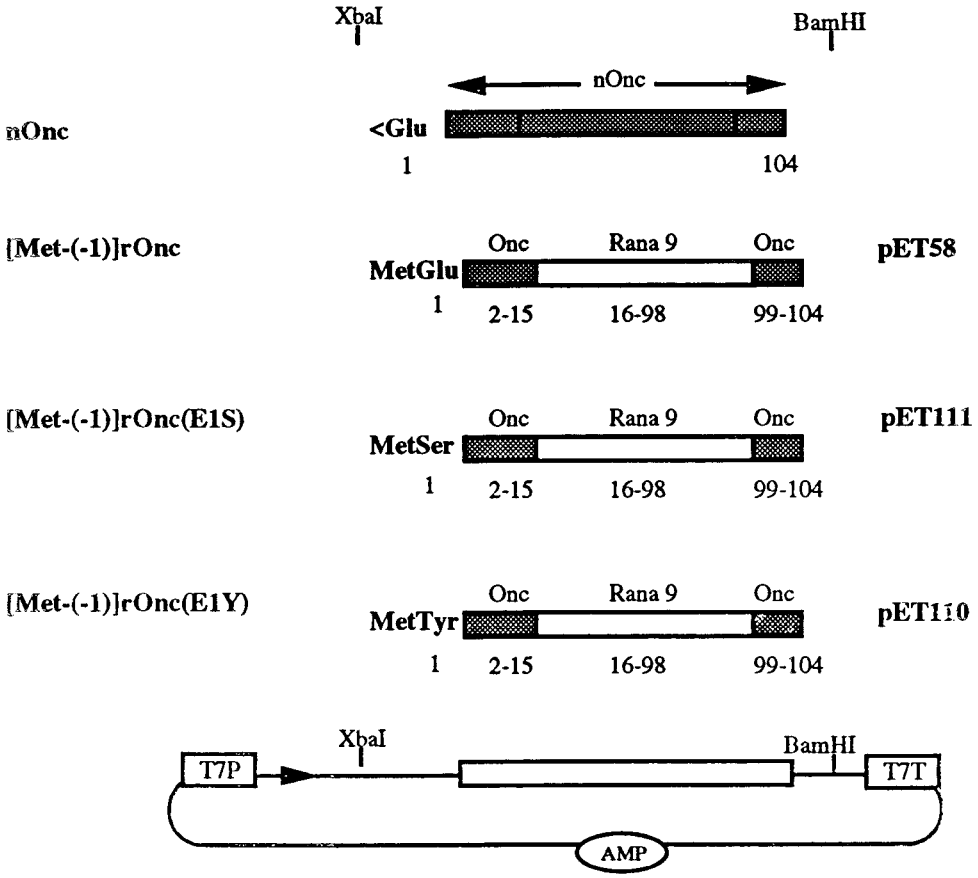

FIGURE 2: Configuration of recombinant DNA constructs compared to nOnc. The PCR product obtained from *Rana pipiens* DNA is identified as Rana 9. The synthetically filled in N- and C-termini are identified as Onc in the constructs encoding [Met-(−1)]rOnc. Corresponding amino acid residues are indicated below each construct. [Met-(−1)]rOnc(E1S) and [Met-(−1)]rOnc(E1Y) differ from rOnc at only the +1 position, as indicated.

otide primers were designed to modify the primary amino acid structure of [Met-(−1)]rOnc by changing the N-terminal amino acid residue following the initiating methionine from glutamic acid to serine ([Met-(−1)]rOnc(E1S)) or tyrosine ([Met-(−1)]rOnc(E1Y)). Thus, the recombinant RNases obtained from the bacteria in this expression system contain an extra methionine at the amino-terminal end ([Met-(−1)]).

The configuration of the DNA encoding recombinant onconase and its derivatives is shown in Figure 2. Amplification of these genes was carried out in a thermal cycler, and the DNA was cloned into an expression vector using methodology previously described (*9*). The plasmids were expressed in BL21(DE3) *E. coli*, and the recombinant proteins were isolated from inclusion bodies as described (*9*) before being applied to a CM-Sephadex C-50 column. Final purification to homogeneity as assessed by gel electrophoresis was achieved by size-exclusion chromatography (Figure 3).

Inhibition of Translation in the Rabbit Reticulocyte Lysate by RNases. Onconase is a potent inhibitor of the translational capacity of the rabbit reticulocyte lysate by a mechanism that depends on degradation of tRNA (*22*). As depicted in Figure 4, the addition of nOnc to the lysate caused protein synthesis inhibition as measured by the incorporation of [^{35}S]-methionine into acid-precipitable protein. Similar to previously reported results, nOnc inhibited protein synthesis with an IC_{50} of 0.36 ng/mL (*6*). [Met-(−1)]rOnc(E1S) and [Met-(−1)]rOnc(E1Y) also inhibited protein synthesis (IC_{50}'s of

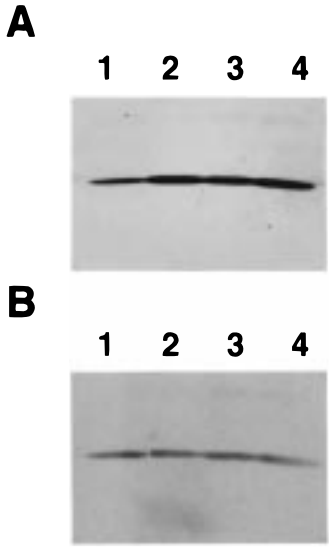

FIGURE 3: SDS−polyacrylamide gel analysis of 1 μg each of nOnc (lane 1), (Met-(−1)]rOnc (lane 2), [Met-(−1)]rOnc(E1S) (lane 3), and [Met-(−1)]rOnc(E1Y) (lane 4). In panel A, the gel is stained with Coomassie blue; in panel B, a Western blot analysis using polyclonal rabbit anti-onconase antibodies is shown.

7.2 and 60 ng/mL, respectively). Although both of these recombinant derivatives were less active than native onconase, they were more effective than [Met-(−1)]rOnc that contains glutamic acid instead of a Ser or Tyr amino acid residue in the +1 position [IC_{50} approximately 100 ng/mL (6)].

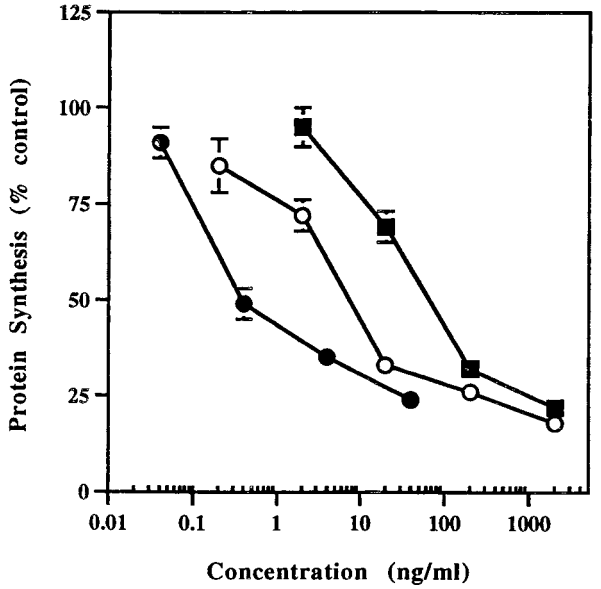

FIGURE 4: Activity of [Met-(−1)]rOnc(E1S) and [Met-(−1)]rOnc-(E1Y) in the rabbit reticulocyte assay compared with nOnc. The two recombinant proteins and nOnc were added to a lysate mixture containing BMV mRNA and [^{35}S]methionine. Protein synthesis was determined by measuring the incorporation of label into newly synthesized proteins as described in Materials and Methods. Data from 4−9 experiments were pooled, averaged, and plotted ±SEM. The results are expressed as a percentage of the control reaction. nOnc, solid circles; [Met-(−1)]rOnc(E1S), open circles; [Met-(−1)]rOnc(E1Y), solid squares.

Since [Met-(−1)]rOnc(E1S) was more potent than [Met-(−1)]rOnc or [Met-(−1)]rOnc(E1Y) in the lysate assay, its RNA specificity was further compared to that of nOnc. Reticulocyte lysates were treated with nOnc or [Met-(−1)]-rOnc(E1S), and an aliquot was removed to determine protein synthesis before total RNA was isolated and analyzed by gel electrophoresis on 10% TBE gels. As shown in Figure 5B, lanes 3−5, nOnc degraded tRNA at concentrations correlating with protein synthesis inhibition (Figure 5A, lanes 3−5), conforming with previously published results (*22*). Similarly, [Met-(−1)]rOnc(E1S) degradation of tRNA correlated with protein synthesis inhibition (compare lanes 6−8 in panels A and B of Figure 5). However, consistent with the results shown in Figure 4, approximately 10-fold more [Met-(−1)]rOnc(E1S) was required. Thus, [Met-(−1)]rOnc-(E1S) retains the tRNA substrate specificity of the native protein in the rabbit reticulocyte lysate assay.

Ribonuclease Activity of Recombinant RNases. The catalytic activity and substrate specificity of recombinant onconase and its derivatives were surveyed using various substrates. In general, nOnc exhibited the highest enzymatic activity, followed by [Met-(−1)]rOnc(E1S) and [Met-(1)]-rOnc(E1Y) (Table 1). Only with poly(A,C) as substrate were [Met-(−1)]rOnc(E1S) and [Met-(−1)]rOnc(E1Y) more active than nOnc. In view of the extremely low activities observed with this synthetic substrate, however, one must be cautious in interpreting this finding. Consistent with previously published results (*23*), nOnc was 13- and 7-fold more active at pH 6.0 than at pH 7.5 with yeast RNA and tRNA, respectively. Yet, [Met-(−1)]rOnc(E1S) and [Met-(−1)]-rOnc(E1Y) lost only 1.6 and 1.5 times the activity with yeast RNA, respectively, and in the case of tRNA, [Met-(−1)]-rOnc(E1S) actually increased in activity with the increase

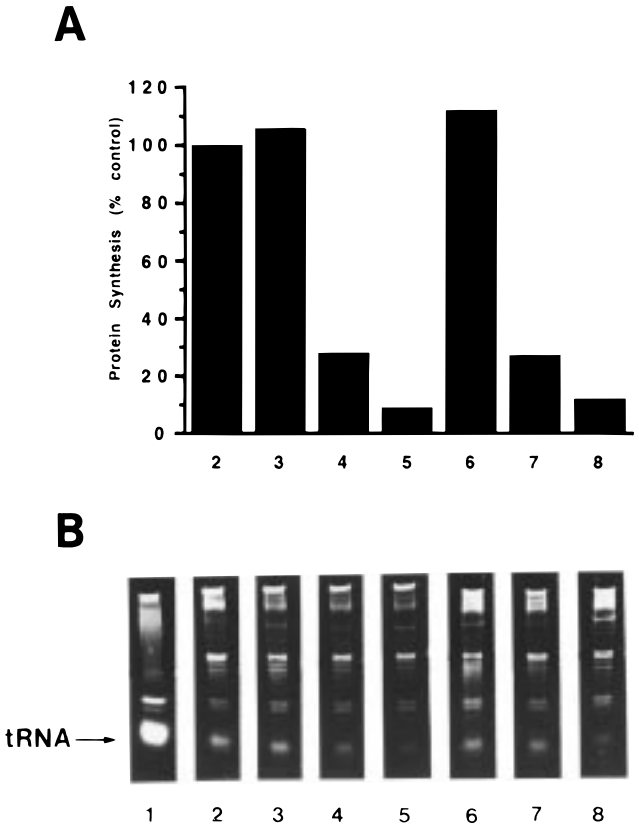

FIGURE 5: Panel A: Inhibition of protein synthesis in reticulocyte lysates by nOnc and [Met-(1)]rOnc(E1S). Lysates were treated as described in the caption to Figure 4 and in Materials and Methods. Lane 2, control lysate without RNase; lanes 3−5, 0.17, 1.7, and 17.0 ng/mL nOnc, respectively; lanes 6−8, 1.7, 17.0, and 170 ng/mL [Met-(−1)]rOnc(E1S), respectively. Panel B: Electrophoresis of RNA from nOnc- and [Met-(−1)]rOnc(E1S)-treated lysates. Reticulocyte RNA was isolated from the treated lysates shown in panel A, as described in Materials and Methods, and electrophoresed on a 10% TBE gel. The RNA samples were stained with ethidium bromide. Lane 1, standard tRNA; lanes 2−8 are as described in panel A.

Table 1: Activity of RNases on Different Substrates[a]

substrate	assay pH	RNase activity (U/mg of protein) nOnc	[Met-(−1)]-rOnc(E1Y)	[Met-(−1)]-rOnc(E1S)
tRNA	6.0	163	<1.0	3.4
tRNA	7.5	24	0.64	15
yeast RNA	6.0	360	0.8	22
yeast RNA	7.5	28	0.5	14
poly(A,C)	7.0	0.0007	0.04	0.01
UpG	6.5	0.27	0.008	0.006
poly(U)	6.5	0.14	0.004	0.02

[a] RNase activity was quantitated as described in Materials and Methods. Units (U) are defined as the changes in absorbance at 260 nm/min calculated from the slopes of the linear part of the assays. Each value is the average of two assays of replicate determinations in separate experiments.

in pH. To further characterize the recombinant onconase derivatives, kinetic studies at pH 7.5 using tRNA as the substrate were performed. As can be seen in Table 2, the affinity of the enzymes for tRNA (K_m) is [Met-(−1)]rOnc-(E1Y) > [Met-(−1)]rOnc(E1S) > nOnc, while the catalytic constant, k_{cat}, increases in the opposite order. As a control, the kinetic parameters for [Met-(−1)]rOnc were also determined and are shown in Table 2. The enzymatic activity of

Table 2: Kinetic Parameters of RNases with tRNA as Substrate[a]

RNase	K_m[b] (μM)	k_{cat}[b] (U mg^{-1})	catalytic efficiency		inhibition by PRI, K_i[c] (M)
			k_{cat}/K_m (U M^{-1} mg^{-1})	%	
nOnc	47	1830	3.9×10^7	100	$\geq 10^{-6}$ [d]
[Met-(−1)]rOnc(E1S)	27	639	2.1×10^7	54	3.1×10^{-11}
[Met-(−1)]rOnc(E1Y)	15	62	0.4×10^7	11	5.4×10^{-11}
[Met-(−1)]rOnc	7100	44	6.2×10^3	0.02	N/A[e]

[a] RNase activity with tRNA as substrate was assayed as described in Materials and Methods. A unit (U) is defined as the absorbance change at 260 nm/min. [b] Apparent k_{cat} and K_m. [c] Calculated from the slope of the Henderson plot (see text and Materials and Methods for detail), using a conversion factor of 1 PRI unit/mL = 6.5×10^{-10} M. [d] (5). [e] N/A, not applicable.

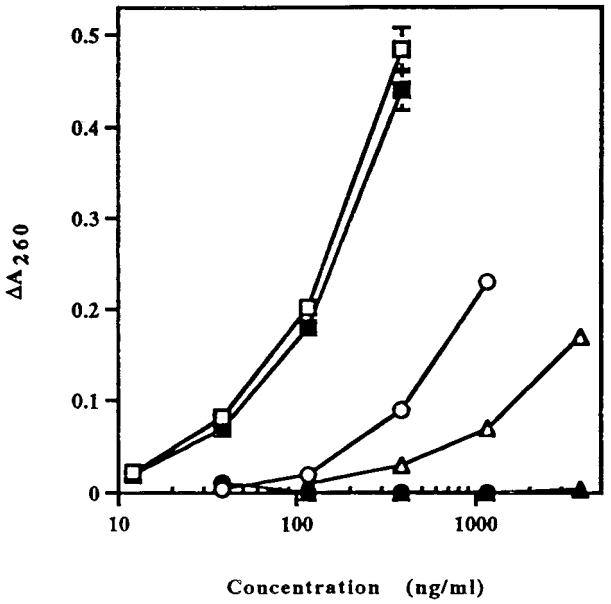

FIGURE 6: Inhibition of RNase activity by PRI. Acid-soluble tRNA fragments were measured as described in Materials and Methods. Assays were performed in the absence of PRI (open symbols) or the presence of 325 U/mL of PRI (solid symbols). The data from a representative experiment are plotted. Standard errors of the means are shown when they are greater than the symbol. nOnc, squares; [Met-(−1)]rOnc(E1S), circles; [Met-(−1)]rOnc(E1Y), triangles.

this species is negligible as evidenced by its low k_{cat} and very large K_m. The k_{cat}/K_m ratio, an indication of catalytic efficiency, confirms that nOnc is the most active. [Met-(−1)]rOnc(E1S) is nearly as efficient as nOnc (54%), and [Met-(−1)]rOnc(E1Y) is only 11% as efficient as nOnc. Thus, the introduction of different amino acid residues into the N-terminal region of onconase can dramatically affect both K_m and k_{cat}.

Inhibition of rOnc Derivatives by the Placental RNase Inhibitor. Human placental RNase inhibitor (PRI) is a specific inhibitor of pancreatic RNase A type enzymes present in cytoplasmic extracts of mammalian tissues (*24*, *25*). PRI inhibits angiogenin and RNase A with K_i values in the 10^{-16}−10^{-13} M range (*26*), although its interaction with onconase is considerably weaker ($\geq 10^{-6}$ M) (*5*). Although we previously determined that [Met-(−1)]rOnc, like onconase, is not significantly inhibited by PRI (*6*), both [Met-(−1)]rOnc(E1S) and [Met-(−1)]rOnc(E1Y) were inhibited by PRI in the rabbit reticulocyte lysate assay (data not shown). Since the lysate assay is a complex mixture, sensitivity to PRI inhibition was more extensively characterized enzymatically using tRNA as the substrate. The data in Figure 6 demonstrate that PRI totally inhibited the RNase activity of [Met-(−1)]rOnc(E1S) and [Met-(−1)]rOnc(E1Y) without affecting the activity of nOnc. Further inhibition studies were performed by varying the tRNA substrate concentrations at several levels of PRI. As shown in Table 2, both [Met-(−1)]rOnc(E1S) and [Met-(−1)]rOnc(E1Y) were inhibited by PRI with K_i values in the 10^{-11} M range.

Cytotoxicity of rOnc Proteins Compared to nOnc in Human Tumor Cell Lines. The cytotoxic effects of [Met-(−1)]rOnc, [Met-(−1)]rOnc(E1S), and [Met-(−1)]rOnc-(E1Y) on SF539 human glioma cells were compared to those of nOnc by measuring the incorporation of [^{14}C]leucine into newly synthesized proteins (Figure 7). Cytotoxicity as assessed by protein synthesis inhibition increased with time after the initial addition of nOnc (IC_{50}'s of 3.5, 0.4, and 0.16 μg/mL after 1, 2, and 5 days, respectively). A similar time-dependent increase in cytotoxicity was observed also with [Met-(−1)]rOnc(E1S) (IC_{50}'s of 10, 3, and 0.35 μg/mL after 1, 2, and 5 days, respectively). As expected, [Met-(−1)]-rOnc containing a methionine in the −1 position was much less active than the native protein. Indeed, no inhibition of protein synthesis by [Met-(−1)]rOnc was observed up to 2 days after the initial addition of the agent. However, protein synthesis was inhibited in SF539 cells after 5 days in the presence of [Met-(−1)]rOnc (IC_{50}, 10 μg/mL) but to a much lesser extent when compared to the native protein (IC_{50}, 0.16 μg/mL) or [Met-(1)]rOnc(E1S)(IC_{50}, 0.35 μg/mL). Inhibition of protein synthesis by [Met-(−1)]rOnc(E1Y) was greater than that caused by [Met-(−1)]rOnc but less than that of the native protein or the serine-containing rOnc derivative (IC_{50}'s of 10, 5, and 2.5 μg/mL after 1, 2, and 5 days, respectively).

Retinoic acid has been shown to disrupt the Golgi apparatus and potentiate the cytotoxicity of several RNases, including that of nOnc in 9L rat (*27*) and U251 human glioma cells (*5*). As shown in Table 3, retinoic acid enhanced the cytotoxicity of both nOnc and [Met-(−1)]rOnc-(E1S) to U251 human glioma cells. Cytotoxicity was increased 5-fold for nOnc (from 21.6 to 4 μg/mL) and >2-fold for [Met-(−1)]rOnc(E1S) (from >1440 to 700 μg/mL). Brefeldin A inhibits vesicular transport from the endoplasmic reticulum (ER) to the Golgi, resulting in a collapse of the *cis* Golgi apparatus, thus blocking the retrograde vesicular transport of vesicles from the Golgi to the ER (*28*, *29*). Table 3 shows that brefeldin A blocked the retinoic acid enhanced activity of nOnc and [Met-(−1)]rOnc(E1S). Activity of nOnc by itself was not blocked by brefeldin A, consistent with previously reported results (*27*). The lysosomotropic amines monensin and NH_4Cl also enhanced the cytotoxicity of nOnc and [Met-(−1)]rOnc(E1S) (Table 3). Monensin enhanced nOnc activity 5.8-fold (from 0.25 to 0.043 μg/mL in the absence and presence of monensin, respectively) and

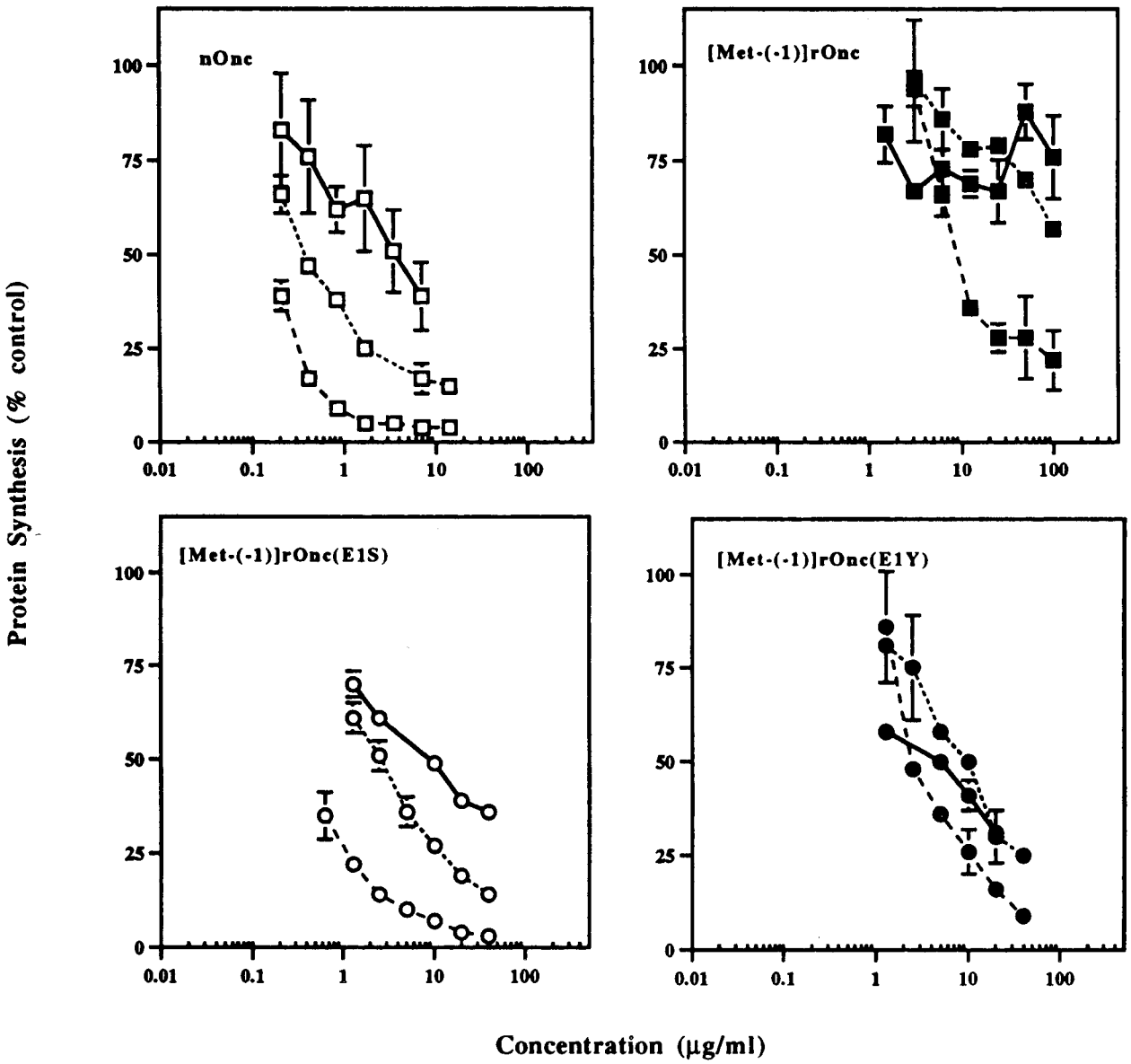

FIGURE 7: Cytotoxicity of nOnc, [Met-(−1)]rOnc, or modified rOnc proteins on SF539 human glioma cells. Cells were plated in individual 96-well microtiter culture plates and treated with varying concentrations of each agent for 1 (solid lines), 2 (dotted lines), or 5 days (dashed lines). Cytotoxicity was determined by measuring the incorporation of [^{14}C]leucine into newly synthesized proteins as described in Materials and Methods. The data shown are representative of five experiments. Standard errors of the means of triplicate determinations are shown when they are greater than the symbol. nOnc, open squares; [Met-(−l)]rOnc, solid squares; [Met-(−1)]rOnc(E1S), open circles; [Met-(−1)]rOnc(E1Y), solid circles.

[Met-(−1)]rOnc(E1S) activity 9.4-fold (from 7.5 to 0.8 μg/mL in the absence and presence of monensin, respectively). NH_4Cl was less effective than monensin in increasing the cytotoxicity of nOnc and [Met-(−1)]rOnc(E1S) (1.8- and 3.8-fold for nOnc and [Met-(−1)r]Onc(E1S), respectively). Similar results were obtained with [Met-(−1)]rOnc(E1Y) (data not shown).

Stability of Recombinant RNases. Since stability in the presence of serum proteins and physiological temperature is important in determining the therapeutic usefulness of a drug, the stability of the rOnc derivatives was compared to that of the native protein. Serial dilutions of serine and tyrosine rOnc derivatives were incubated in serum-containing medium at 37 °C for 2 and 4 days and compared to freshly prepared serial dilutions of the proteins (0 days, Figure 8, solid symbols). The native protein, as well as the two recombinant derivatives, retained full cytotoxic activity even after 4 days. Additionally, the stability was assessed in the presence of cultured tumor cells in serum-containing medium to determine whether the recombinant derivatives were less stable under in vitro cell culture conditions (Figure 8, open symbols). Even under these conditions, as seen in Figure 8, there was no significant change in the IC_{50}'s of native or recombinant Oncs, irrespective of prior incubation with the cultured cells.

Tritiated RNase A is catabolized with a half-life of 75 h in cell culture, and the degradation is enhanced 2-fold in response to serum deprivation (*19*). To directly examine the proteolysis of native Onc in comparison to the serine-containing analogue, the proteins were tritiated and added to cultured SF539 cells. The percentages of radioactive protein remaining (acid insoluble) after 24 and 72 h were 99% for nOnc and 98% for [Met-(−1)]rOnc(E1S) in the presence of serum and 99% and 98% after 24 and 48 h in

Table 3: Enhancement of RNase in Vitro Cytotoxic Activity[a]

RNase	additions	IC_{50}, μg/mL	fold increase
nOnc[b]	none	0.25	
	monensin	0.04	5.8
	NH_4Cl	0.14	1.8
[Met-(−1)]rOnc(E1S)[b]	none	7.50	
	monensin	0.80	9.4
	NH_4Cl	2.00	3.8
nOnc[c]	none	21.60	
	retinoic acid	4.00	5.4
	retinoic acid + BFA	22.80	1.0
[Met-(−1)]rOnc(E1S)[c]	none	>1440	
	retinoic acid	700	>2.0
	retinoic acid + BFA	>1440	1.0

[a] Cells were plated into 96-well microtiter plates and treated with nOnc or [Met-(−1)]rOnc(E1S) as described in Materials and Methods. [b] Either 0.12 μM monensin, 10 mM NH_4Cl, or buffer was included, and the cells (SF539 human glioma cells) plus additions were incubated for 3 days. [c] Either 10 μM retinoic acid or 10 μM retinoic acid plus 4 μg/mL BFA was included, and the cells (U251 human glioma cells) were incubated for 48 h in the absence of serum. Protein synthesis was determined as described in Materials and Methods.

the absence of serum. These results indicate that both native and recombinant forms of Onc are more stable in cell culture than RNase A and virtually indistinguishable among themselves with regard to the three methods used to detect stability.

DISCUSSION

Analysis of the structure of nOnc reported by Mosimann et al. (*4*) showed that the N-terminal region folds back over the active site region, with the carbonyl group of the N-terminal pyroglutamate being involved in a hydrogen bond network together with several active site residues. In this regard, the importance of these N-terminal interactions were demonstrated in previous studies that showed that rOnc expressed as a [Met-(−1)] fusion protein containing either Glu (*5*,*6*) or Gln(*5*) in the +1 position had markedly less enzymatic and cytotoxic activities. Taken together, these results suggested that the introduction of a hydroxyl-containing amino acid could mimic the carbonyl group on ⟨Glu. Of the three OH-containing natural amino acids (Thr, Ser, and Tyr), the smallest and most flexible (Ser) and the bulkiest (Tyr) were chosen to be introduced at the N-terminal position following the initiating methionine. Although both rOncs regained nOnc-like activities, the Ser1-containing derivative with a catalytic efficiency approaching that of nOnc was more potent than the tyrosine analogue in all of the assays. This is most likely due to the flexibility of the small serine amino acid residue that would allow the formation of multiple isoforms, some of which could form optimal H-bonds with the active site residues. Conversely, the bulkiness of the Tyr1 amino acid residue would limit the number of possible isoforms. The resulting structure, according to our model, would present less than optimal H-bonding for Tyr1 which could explain the lower catalytic efficiency of this recombinant derivative.

Although both of the recombinant onconase analogues were enzymatically active, the RNA substrate profile was not identical to that of nOnc in assays in which the ribonucleolytic activity on single substrates was examined. For at least one substrate, tRNA, the recombinant onconase derivatives were more active at pH 7.5 than at pH 6.0; the opposite was true for nOnc. With yeast RNA, the loss in activity that occurred when the pH was increased to 7.5 was greater for nOnc than for [Met-(−1)]rOnc(E1S) or [Met-(−1)]rOnc(E1Y). In a more complex environment such as the rabbit reticulocyte lysate assay, however, the ribonucleolytic profile of [Met-(−1)]rOnc(E1S) was similar to that of nOnc. Both RNases inhibited protein synthesis in the rabbit reticulocyte lysate concomitant with degradation of tRNA, an activity characteristic of native onconase (*22*). For this reason the degradative activity observed in the lysate may be more predictive of the proper RNA substrate profile for nOnc and its derivatives since it may represent a more natural environment for the enzymes. Thus, we chose tRNA as the preferred substrate when further characterizing and comparing enzymatic activities.

Interestingly, substitution of a single amino acid residue (either serine or tyrosine) at position 1 rendered both of those analogues sensitive to inhibition by PRI. Superposition of nOnc on the RNase A component of the PRI−RNase A complex (*11*) shows interesting features. Onconase is a smaller protein than RNase A, and some regions which are present in RNase A and absent in onconase are involved in interactions with PRI. In particular, the N-terminus of RNase A is extended, while in onconase it makes a turn, "closing" the structure of onconase on itself. Moreover, the N-terminal ⟨Glu, which in fact does not possess a free N-terminal group, is directly H-bonded to the phosphate in the active site, and also to Lys9, through its carbonyl oxygen. In the complexes with PRI, Lys9 of nOnc keeps its H-bond with ⟨Glu, while in the recombinant enzymes it H-bonds to the C-terminal Ser456 of PRI. The C-terminal group of PRI has also been described to form contacts with the N-terminal region of RNase A (*11*), and the equivalent residue in PRI (hRI), C-terminal Ser460, is also involved in H-bonds with the N-terminal region of angiogenin (*30*). The presence of Met-(−1) in the recombinant enzymes is yet another factor that should be taken into account. According to our model, the N-terminal group of Met(−1) forms an H-bond with the phosphate in the active site; yet other arrangements of the residue would be possible, and it is difficult to speculate about its role without further structural data.

In our model, Lys31, which is part of the active site, is in all cases forming an H-bond with Asp431 of PRI. It should be noted, however, that the X-ray structure of nOnc, which served as the starting point for our modeling, presented Lys31 pointing out of the active site in what would be a nonactive form of the enzyme, and therefore the contact with PRI is favored in our model. However, the situation in nOnc, with ⟨Glu1 and Lys9 forming a H-bond, may provide an opportunity for Lys31 to remain "nested" inside the RNase molecule, while in the recombinant forms, Lys31 could bind to PRI more easily. The equivalent residue to Lys31 in angiogenin, Lys40, is H-bonded to PRI in the structure of the complex (*30*). Other residues from onconase forming H-bonds with PRI in our model are Asp20, Asp32, and Arg73. Thus, the introduction of a Met-(−1) residue in the rOnc proteins could favor a much more open arrangement of the N-terminal regions, allowing some residues to interact with the inhibitor. In our model, Lys9 (H-bonded to ⟨Glu in nOnc) would easily H-bond to the inhibitor, while the amino acid present in position 1 would

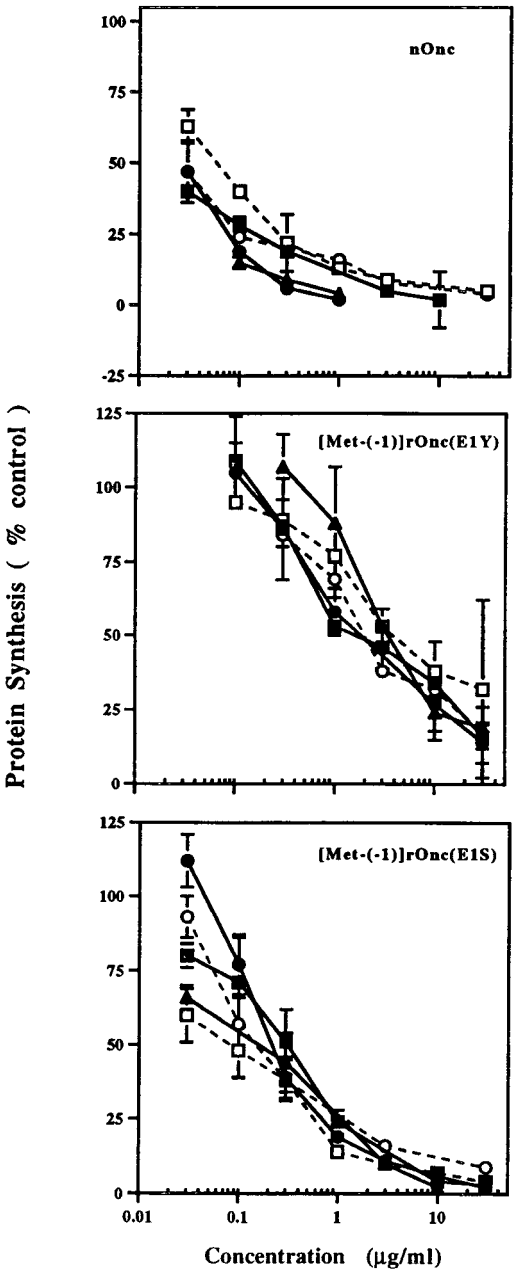

FIGURE 8: Stability of nOnc and modified rOnc proteins in the presence of serum without and with the presence of cells. Concentration curves of nOnc (top panel), [Met-(−1)]rOnc(E1Y) (middle panel), and [Met-(−1)]rOnc(E1S) (bottom panel) were made in the presence of media containing 10% fetal bovine serum and incubated at 37 °C for 1, 2, and 4 days such that all solutions could be tested at the same time. SF539 human glioma cells were plated out into 96-well microtiter plates and treated with the preincubated solutions for 3 days before being pulsed with [^{14}C]-leucine and harvested as described in Materials and Methods. The data shown are representative of two experiments (solid lines and solid symbols: squares, 1 day; circles, 2 days; triangles, 4 days). In the second type of experiment, SF539 cells were treated with the indicated concentrations of nOnc or one of the modified rOncs. Medium containing the diluted samples was then removed and applied to another plate of fresh cells. After 3 days, plates were then pulsed with [^{14}C]leucine for 2−4 h, harvested and counted as described in Materials and Methods (open symbols and dashed lines: squares, fresh dilution curve; circles, media containing dilutions of nOnc and recombinant proteins previously incubated with cells). Standard errors of the means of triplicate determinations are shown when they are greater than the symbol.

basically be responsible for changes in catalytic activity.

In addition to exhibiting ribonuclease activity, both [Met-(−1)]rOnc(E1S) and [Met-(−1)]rOnc(E1Y) retained substantial cytotoxic activity, but not the full cytotoxic activity of native onconase. After 24 h, both of the onconase analogues were about 3-fold less active than the native protein on cultured SF539 human glioma cells. However, after an additional 4 days in the presence of these agents, the relative activity of [Met-(−1)]rOnc(E1Y) decreased (16-fold less active than the native protein), while [Met-(−1)]-rOnc(E1S) slightly increased its relative activity (about 2-fold less active than the native protein). Since onconase cytotoxicity correlates with its ribonuclease activity (*3*), a likely explanation for these results is the diminished enzymatic activity of the two recombinant derivatives. To test this assumption, other possibilities were considered, such as PRI sensitivity and differences in intracellular routing or stability.

The relative insensitivity of onconase to PRI has been postulated to contribute to its cytotoxicity. Yet [Met-(−1)]-rOnc(E1S) and [Met-(−1)]rOnc(E1Y) were only about 2−20-fold less cytotoxic than nOnc, while their sensitivity to PRI increased $>10^5$ fold. Similar findings have been reported for chimeras between EDN (*6*) or human pancreatic RNase (rhRNase) (*5*) and rOnc. Though the EDN−rOnc hybrid protein was inhibited by PRI, it was at least as cytotoxic as the PRI-insensitive nOnc in certain cell lines (*6*). Also, two hybrid rhRNase proteins were equally cytotoxic to cells, even though one of the hybrids was 100 000 times more sensitive to inhibition by PRI (*5*). Taken together, these findings raise questions about the role and importance of PRI inhibition in RNase cytotoxicity.

Internalization and routing have been reported to be instrumental in the mechanism of onconase cytotoxicity (*27*). Monensin and NH_4Cl raise endosomal pH in cells and markedly influence the cytotoxicity of diphtheria toxin and ricin immunotoxins as reviewed in ref *31* and *32*. Both monensin and NH_4Cl block diphtheria toxin activity but markedly enhance the activity of ricin. Consistent with previously published results (*21*), monensin potentiation of onconase activity is greater than the potentiation elicited by NH_4Cl. The same pattern of enhancement was observed with [Met-(−1)]rOnc(E1S), suggesting that a common route of internalization is used by both proteins. Moreover, the two proteins appear to be similarly routed into the cytosol. In the presence of retinoic acid, the Golgi apparatus is disrupted and onconase cytotoxicity is increased (*27*). This indicates that onconase can reach the cytosol more efficiently through a disrupted Golgi apparatus. When retinoic acid is combined with BFA, potentiation of onconase activity is blocked (*27*). BFA causes a collapse of the *cis* Golgi apparatus, inhibiting vesicular transport from the *cis* Golgi to the endoplasmic reticulum (*28*, *29*). Yet BFA does not block onconase cytotoxicity in the absence of retinoic acid, indicating that the normal intracellular routing of onconase is different from that induced by retinoic acid (*27*). In all of these respects, in the presence of retinoic acid and retinoic acid combined with BFA, the activity of [Met-(−1)]rOnc(E1S) qualitatively mimics that of the native protein, indicating that both proteins also route to the cytosol via the same pathway.

We have also examined whether the substitution of Ser1 or Tyr1 for ⟨Glu1 might have affected the stability of the recombinant onconase analogues. Moreover, since stability

is an important characteristic for any drug, this parameter was examined by using three different methods. Stability at 37 °C was tested by preincubating dilutions of nOnc and the two recombinant proteins in the absence and presence of cultured SF539 human glioma cells followed by the application of the preincubated dilution curve media to new cultures of SF539 cells. Parallel wells contained fresh (not preincubated) dilution curve media. Since onconase is internalized (*21, 27*), the possibility of proteolytic degradation in cultured cells existed. Thus, this possibility was even more rigorously examined by determining the percentage of tritiated nOnc or tritiated [Met-(−1)]rOnc(E1S) (acid-insoluble cpm) remaining in cultures after 1 or 3 days. Under all of these assay conditions, the recombinant analogues were indistinguishable from the native protein. Furthermore, all three proteins were more stable under these conditions (half-life > 72 h) than the previously published half-life of tritiated RNase A (half-life = 75 h) (*19*). Resistance to intracellular degradation may be a factor in determining RNase cytotoxic potential.

Since onconase, combined with tamoxifen, is being evaluated in Phase III clinical trials in patients with pancreatic cancer (S. Mikulski, personal communication), it is approaching maturity as a new member of the arsenal of anticancer drugs. Future generations of onconase-based drugs could be designed if DNA encoding an active protein were available. For example, onconase conjugated to antibodies was more potent toward tumor cells than native unconjugated onconase (*8*). Onconase was linked to antibodies via disulfide or thioether bonds using bifunctional cross-linking agents that reacted with lysine amino groups. Since the sites of derivatization and linkage were not controlled, the conjugates were heterogeneous. That the conjugation process itself impairs onconase conjugate activity is a common phenomenon in conjugating protein toxins, as reviewed in ref *33*. Engineering cysteine residues on the surface of recombinant onconase could be expected to alleviate nonspecific modification, thereby enhancing the activity of the conjugate (*34*−*37*).

To avoid the heterogeneity of chemical conjugates, recombinant fusion proteins have been made by fusing DNA encoding specific cell binding ligands such as single-chain (sFv) antibodies to toxins. Single-chain antibody toxin fusion proteins are smaller than their IgG counterparts and may be advantageous for penetration of solid tumors (see ref *38* and references therein). In this regard, other members of the pancreatic RNase family have been shown to form potent immunotoxins when genetically linked to antibodies that specifically recognize tumor-associated antigens (*9, 39*−*41*). Since onconase is a chemosensitizer (*42, 43*), even in MDR1 (P-glycoprotein-mediated) drug-resistant colon cancer cells (*44*), it may be an especially attractive candidate for targeting solid carcinomas as a fusion protein. The results presented here demonstrate that rational design of new onconase genes is feasible and productive.

ACKNOWLEDGMENT

We are grateful for the outstanding technical help of Dale Ruby and appreciate the helpful discussions with Dr. Hsiang-fu Kung. We also thank Mrs. Ann Rogers for excellent help in the preparation of this manuscript. We acknowledge the Frederick Biomedical Supercomputer Center for the use of its facilities. The contents of this publication do not necessarily reflect the views or policies of the Department of Health and Human Services, nor does mention of trade names, commercial products, or organizations imply endorsement by the U.S. Government.

REFERENCES

1. Darzynkiewicz, Z., Carter, S. P., Mikulski, S. M., Ardelt, W. J., and Shogen, K. (1988) *Cell Tissue Kinet. 21*, 169−182.
2. Mikulski, S. M., Ardelt, W., Shogen, K., Bernstein, E. H., and Menduke, H. (1990) *J. Natl. Cancer Inst. 82*, 151−153.
3. Ardelt, W., Mikulski, S. M., and Shogen, K. (1991) *J. Biol. Chem. 266*, 245−251.
4. Mosimann, S. C., Ardelt, W., and James, M. N. G. (1994) *J. Mol. Biol. 236*, 1141−1153.
5. Boix, E., Wu, Y. N., Vasandani, V. M., Saxena, S. K., Ardelt, W., Ladner, J., and Youle, R. J. (1996) *J. Mol. Biol. 257*, 992−1007.
6. Newton, D. L., Xue, Y., Boque, L., Wlodawer, A., Kung, H. F., and Rybak, S. M. (1997) *Protein Eng. 10*, 463−470.
7. Mikulski, S. M., Grossman, A. M., Carter, P. W., Shogen, K., and Costanzi, J. J. (1993) *Int. J. Oncol. 3*, 57−64.
8. Rybak, S. M., Newton, D. L., Mikulski, S. M., Viera, A., and Youle, R. J. (1993) *Drug Delivery 1*, 3−10.
9. Newton, D. L., Xue, Y., Olsen, K. A., Fett, J. W., and Rybak, S. M. (1996) *Biochemistry 35*, 545−553.
10. Cambillau, C., and Horjales, E. (1987) *J. Mol. Graph. 5*, 174−177.
11. Kobe, B., and Deisenhofer, J. (1995) *Nature 374*, 183−186.
12. Brunger, A. (1992) *XPLOR: A System for X-ray Crystallography and NMR*, Yale University Press, New Haven.
13. Horten, R. M., Cai, Z., Ho, S. N., and Pease, L. R. (1990) *BioTechniques 8*, 528−535.
14. St. Clair, D. K., Rybak, S. M., Riordan, J. F., and Vallee, B. L. (1987) *Proc. Natl. Acad. Sci. U.S.A. 84*, 8330−8334.
15. DePrisco, R., Sorrentino, S., Leone, E., and Libonati, M. (1984) *Biochim. Biophys. Acta 788*, 356−363.
16. Libonati, M., and Floridi, A. (1969) *Eur. J. Biochem. 8*, 81−87.
17. Cleland, W. W. (1979) *Methods Enzymol. 63*, 103−138.
18. Henderson, P. J. F. (1972) *Biochem. J. 127*, 321−333.
19. Backer, J. M., Bourret, L., and Dice, J. F. (1983) *Proc. Natl. Acad. Sci. U.S.A. 80*, 2166−2170.
20. Rybak, S. M., Saxena, S. K., Ackerman, E. J., and Youle, R. J. (1991) *J. Biol. Chem. 266*, 21202−21207.
21. Wu, Y. N., Mikulski, S. M., Ardelt, W., Rybak, S. M., and Youle, R. J. (1993) *J. Biol. Chem. 268*, 10686−10693.
22. Lin, J. J., Newton, D. L., Mikulski, S. M., Kung, H. F., Youle, R. J., and Rybak, S. M. (1994) *Biochem. Biophys. Res. Commun. 204*, 156−162.
23. Ardelt, W., Lee, H. S., Randolph, G., Viera, A., Mikulski, S. M., and Shogen, K. (1994) *Protein Sci. 3, Suppl. 1*, 137.
24. Blackburn, P., and Moore, S. (1982) *The Enzymes 15*, 317−433.
25. Blackburn, P., Wilson, G., and Moore, S. (1977) *J. Biol. Chem. 252*, 5904−5910.
26. Lee, F. S., Auld, D. S., and Vallee, B. L. (1989) *Biochemistry 28*, 219−224.
27. Wu, Y. N., Saxena, S. K., Ardelt, W., Gadina, M., Mikulski, S. M., DeLorenzo, C., D'Allessio, G., and Youle, R. J. (1995) *J. Biol. Chem. 270*, 17476−17481.
28. Doms, R. W., Russ, G., and Yewdell, J. W. (1989) *J. Cell. Biol. 109*, 61−72.
29. Lippincott-Schwartz, J., Yuan, L. C., Bonfacino, J. S., and Klausner, R. D. (1989) *Cell 56*, 801−813.
30. Papageorgiou, A. C., Shapiro, R., and Acharya, H. R. (1997) *EMBO J.* 16, 5162−5177.
31. Casellas, P., and Jansen, F. K. (1988) in *Immunotoxins* (Frankel, A. E., Ed.) pp 351−369, Kluwer Academic Publishers, Boston.

32. Johnson, V. G., and Youle, R. J. (1991) in *Intracellular Trafficking of Proteins* (Steer, C. J., and Hanover, J. A., Eds.) pp 183−225, Cambridge University Press, Cambridge.
33. Wawrzynczak, E. J., and Thorpe, P. E. (1988) in *Immunotoxins* (Frankel, A. E., Ed.) pp 239−251, Kluwer Academic Publishers, Boston.
34. Bernhard, S. L., Better, M., Fishwild, D. M., Lane, J. A., Orme, A. E., Garrison, D. A., Birr, C. A., Lei, S. P., and Carroll, S. F. (1994) *Bioconjugate Chem. 5*, 126−132.
35. Better, M., Bernhard, S. L., Fishwild, D. M., Nolan, P. A., Bauer, R. J., Kung, A. H., and Carroll, S. F. (1994) *J. Biol. Chem. 269*, 9644−9650.
36. Kreitman, R. J., Puri, R. K., Leland, P., Lee, B., and Pastan, I. (1994) *Biochemistry 33*, 11637−11644.
37. Lappi, D. A., Matsunami, R., Martineau, D., and Baird, A. (1993) *Anal. Biochem. 212*, 446−451.
38. Brinkmann, U., and Pastan, I. (1994) *Biochim. Biophys. Acta 1198*, 27−45.
39. Deonarain, M. P., and Epenetos, A. A. (1995) *Tumor Targeting 1*, 177−182.
40. Newton, D. L., Nicholls, P. J., Rybak, S. M., and Youle, R. J. (1994) *J. Biol. Chem. 269*, 26739−26745.
41. Rybak, S. M., Hoogenboom, H. R., Meade, H., Raus, J. C. M., Schwartz, D., and Youle, R. J. (1992) *Proc. Natl. Acad. Sci. U.S.A. 89*, 3165−3169.
42. Mikulski, S. M., Viera, A., Ardelt, W., Menduke, H., and Shogen, K. (1990) *Cell Tissue Kinet. 23*, 237−246.
43. Mikulski, S. M., Viera, A., and Shogen, K. (1992) *Int. J. Oncol. 1*, 779−785.
44. Rybak, S. M., Pearson, J. W., Fogler, W. F., Volker, K., Spence, S. E., Newton, D. L., Mikulski, S. M., Ardelt, W., Riggs, C. W., Kung, H. F., and Longo, D. L. (1996) *J. Natl. Cancer Inst. 88*, 747−753.

BI972147H